Bioelectrochemistry 75 (2009) 37–43

Contents lists available at ScienceDirect

Bioelectrochemistry

journal homepage: www.elsevier.com/locate/bioelechem

Electrochemical DNA biosensor for the detection of DNA hybridization with the amplification of Au nanoparticles and CdS nanoparticles

Ping Du, Hongxia Li, Zhenhua Mei, Shufeng Liu *

Key Laboratory of Eco-chemical Engineering, Ministry of Education; College of Chemistry and Molecular Engineering, Qingdao University of Science and Technology, Qingdao 266042, China

ARTICLE INFO

Article history:
Received 18 September 2008
Received in revised form 14 January 2009
Accepted 15 January 2009
Available online 27 January 2009

Keywords:
Au nanoparticles
CdS nanoparticles
Voltammetry
DNA hybridization
DNA biosensor

ABSTRACT

In this article, colloidal gold nanoparticles (Au NPs) and carboxyl group-functionalized CdS Nanoparticles (CdS NPs) were immobilized on the Au electrode surface to fabricate a novel electrochemical DNA biosensor. Both Au NPs and CdS NPs, well known to be good biocompatible and conductive materials, could provide larger surface area and sufficient amount of binding points for DNA immobilization. Cyclic voltammetry (CV) and electrochemical impedance spectroscopy (EIS) experiments were performed to follow the whole electrode fabrication process. DNA immobilization and hybridization were characterized with differential pulse voltammetry (DPV) by using $[Co(phen)_2(Cl)(H_2O)]Cl{\cdot}2H_2O$ as an electrochemical hybridization indicator. With this approach, the target DNA could be quantified at a linear range from 2.0×10^{-10} to 1.0×10^{-8} M, with a detection limit of 2.0×10^{-11} M by 3σ. In addition, the biosensor exhibited a good repeatability and stability for the determination of DNA sequences.

1. Introduction

DNA biosensors for the detection of nucleic acid sequences have attracted ever increasing interests in connection with highly demanding research efforts directed to gene analysis, clinical disease diagnosis, or even forensic applications [1–5]. Various techniques including optical, electrochemistry, surface plasmon resonance spectroscopy, and quartz crystal microbalance, etc have been well developed for DNA detection [6–9]. Among them, electrochemistry offer great advantages such as simple, rapid, low-cost and high sensitivity [10]. A key issue faced with any DNA hybridization biosensor is the immobilization amount and accessibility of probe DNA for hybridization recognition [11–14]. Increasing the immobilization amount and controlling over the molecular orientation of probe DNA would markedly improve the performance properties of DNA biosensor. In order to achieve this goal, nanomaterials could be used as an elegant solution for the control of DNA immobilization and hybridization. For a decade, metal and semiconductor nanoparticles have shown huge potential in the fields of biosensing, diagnostics and molecular therapeutics because of its excellent optical and electrical properties [15–18].

Owing to the large surface area and biocompatibility with biosystem, gold nanoparticles (Au NPs) have been shown as a good candidate for enhancement of DNA immobilization and hybridization and they have been directly linked onto the biosensor surface via various strategies such as covalent linking, electrodeposition, electroless deposition, sol–gel, etc [19–22] Semiconductor nanoparticles conjugated with various biomolecules such as DNA, protein, etc have been also widely applied to the detection of biosensing event by, especially optical, electrochemical, electrochemiluminescence, photoelectrochemical means [23,24]. Wang et al. [25] employed semiconductor nanoparticles to develop an electrochemical coding technology for simultaneous detection of multiple DNA targets. They also [26] developed a potentiometric sensor for DNA hybridization detection by the use of semiconductor nanoparticles label. Willner et al. used semiconductor nanoparticles to construct a series of new electrochemical and photoelectrochemical biosensors for various biosystems assays [27–30]. Jie et al. [31] adopted CdS nanoparticles to construct a novel electrochemiluminescence biosensor for the detection of low-density lipo-protein (LDL). Li et al. [32] developed a label-free DNA sensor for sequence-specific DNA detection based on silicon nanowires. Liang et al. [33] used tin oxide nanoparticle to build up a photoelectrochemical sensor for DNA oxidation damage. Whereas, most of these research efforts focused on developing the novel detection strategy by semiconductor nanoparticles. As for the key element involved in the biosensor fabrication, the ability of DNA immobilization and hybridization on semiconductor surface, unfortunately, till now, no much works were reported to concentrate on this primary and important event.

In this paper, the DNA biosensor surface was fabricated with the sequential modification of Au NPs and CdS NPs. Au NPs were firstly assembled on the electrode surface by its electrostatic interaction with cysteamine. The modified Au NPs were used to increase the electrode surface area for more binding amount of CdS and finally enhance the electrochemical responses. The further CdS NPs modification was

* Corresponding author. Tel./fax: +86 532 84022750.
E-mail address: sliu@qust.edu.cn (S. Liu).

1567-5394/$ – see front matter © 2009 Elsevier B.V. All rights reserved.
doi:10.1016/j.bioelechem.2009.01.003

carried out by a simple covalent linking method of carboxyl acid group functionalized CdS NPs with amino group of cysteine. The DNA immobilization and hybridization on the exterior CdS NPs was characterized with the use of $Co(phen)_2^{2+}$ as an electrochemical indicator. The developed electrochemical DNA biosensor based upon the Au NPs and CdS NPs was convinced to hold a potential for the further application of metal and semiconductor nanoparticles in DNA detection.

2. Experimental

2.1. Materials

All of synthetic oligonucleotides were purchased from SBS Genetech. Co. Ltd. (China). Their base sequences are as follows:

capture ssDNA sequence: 5′-NH_2-CGA-CAG-TGG-TCC-CAA-AGA-3′
target ssDNA sequence: 5′-TCT-TTG-GGA-CCA-CTG-TCG-3′
one-base mismatched sequence: 5′-TCT-TTG-GGA-CCA-GTG-TCG-3′
non-complementary sequence: 5′-CAT-TAG-AGA-TGG-GGA-CGA-3′

All 18-base oligonucleotide stock solutions (1.0 μM) were prepared using 10 mM pH 7.0 PBS solutions and were stored at 4 °C.

1-Ethyl-3-(3-dimethylaminopropyl) carbodiimide (EDC) was purchased from Sigma (USA). Chloroauric acid tetrahydrate were obtained from Sinopharm Chemical Reagent Co., Ltd. (China). Mercaptoacetic acid was obtained from Yuanhang Chemical Company (China). Cadmium chloride hemidihydrate and Sodium sulfide nonahydrate were purchased from Bodi Chemical Reagent Co., Ltd. (China).

All the reagents were analytical grade and used without further purification. Doubly distilled water was used throughout.

2.2. Apparatus

A CHI 832b electrochemical analyzer (Shanghai CH Instrument Company, China) connected to a modified Au working electrode, an Ag/AgCl reference electrode, and a platinum-wire auxiliary electrode, was used for the electrochemical measurement. All potentials are reported versus Ag/AgCl reference electrode at room temperature. The solution pH was measured with a model PHS-25 digital acidimeter (Shanghai Leici Factory, China).

2.3. Au NPs preparation

Gold nanoparticles were prepared according to the reference [34] reported previously with a slight modification. 3.0 mL of 1% trisodium citrate was added to 100 mL solution containing 0.01 g $HAuCl_4 \cdot 4H_2O$ and stirred for 40 min at the boiling point. Then, they were left to cool to room temperature. The prepared gold nanoparticles have an average diameter of approximately 24 nm as characterized by TEM (Fig. 1a).

2.4. Water soluble CdS NPs preparation

Mercaptoacetic acid-capped CdS NPs were prepared according to the literature [35]. A 2 μL sample of mercaptoacetic acid was added to 100 mL of 11 mM cadmium chloride solution under vigorous stirring, and the pH was adjusted to 11 with 0.5 M NaOH aqueous solution. After purging the solution with nitrogen gas for 30 min, 50 mL of 1.34 mM Na_2S aqueous solution was added dropwise. The reaction was then kept under bubbling nitrogen for 24 h. The resulting nanoparticles have an average diameter of 20 nm (Fig. 1b).

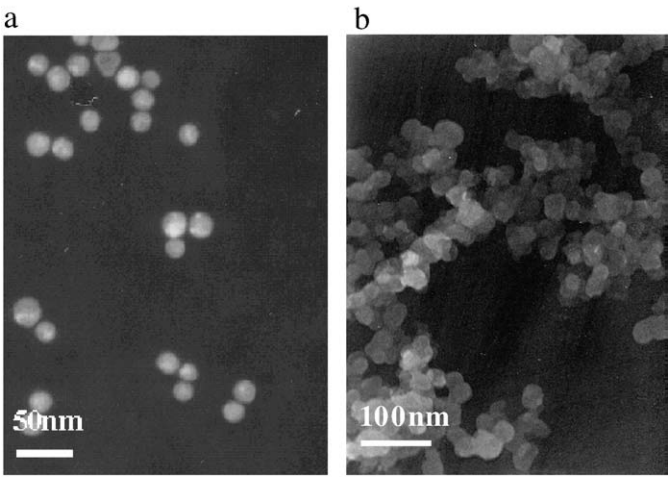

Fig. 1. The SEM image of the Au nanoparticles and CdS nanoparticles.

2.5. Electrode surface modification

The Au electrode surface was freshly polished prior to use sequentially with 1, 0.3, and 0.05 μm α-Al_2O_3 paste, and rigorously rinsed with doubly distilled water following each polish. The polished electrode was then cleaned ultrasonically sequentially in water and 95% ethanol for 3 min. Before surface modification, the bare electrode was scanned in 0.5 M H_2SO_4 between 0.3 and 1.5 V until a reproducible cyclic voltammogram (CV) was obtained. The self-assembly of cysteamine was accomplished with the immersion of Au electrode into 0.02 M deoxygenated cysteamine aqueous solution for 20 h in darkness at room temperature. Then, the electrode was rinsed thoroughly with doubly distilled water and dipped into the colloidal gold solution at 4 °C for 10 h. To assemble the CdS NPs onto the electrode, the gold nanoparticles modified electrode was firstly immersed in 0.02 M cysteine solution at 4 °C for 20 h, followed by soaking in 40 μL of 0.05 mM CdS NPs containing 20 mg mL^{-1} EDC at 4 °C for 2 h. Schematic diagram of the biosensor fabrication was shown as Fig. 2.

2.6. The immobilization of the ssDNA on the modified electrode surface

The probe DNA immobilization was performed with the modified electrode incubated into 1.0×10^{-5} M probe DNA in 10 mM PBS solution containing 0.1 M EDC for 2 h at room temperature under gently stirring. Finally, the immobilized electrode was rinsed with PBS buffer solution (pH = 7.0) containing 0.1% SDS and stored at 4 °C for the hybridization.

2.7. The hybridization of probe DNA modified electrode with target DNA

The hybridization experiments were carried out by immersing the probe DNA immobilized electrode into different concentrations of target DNA sequence in 10 mM PBS buffer solution (pH = 7.0) for 40 min at 40 °C. And then, the hybridized electrodes were rinsed with PBS buffer solution (pH = 7.0) containing 0.1% SDS buffer solution.

2.8. Electrochemical measurement using $Co(phen)_2^{2+}$ as the electrochemical indicator

The DNA modified electrodes were firstly incubated into 0.1 mM $Co(phen)_2^{2+}$ in 0.2 M Tris–HCl aqueous solution (pH = 6.8) for 30 min. Then, the electrodes were taken out and rinsed with water, and subjected to electrochemical experiments in a 0.2 M Tris–HCl aqueous solution (pH = 6.8) containing no indicator. The DPV experiments were executed with the following parameters: the initial potential was −0.20 V; the high potential was 0.60 V; the low potential was −0.20 V; the pulse amplitude was 0.05 V; the pulse period was 0.2 s; and the

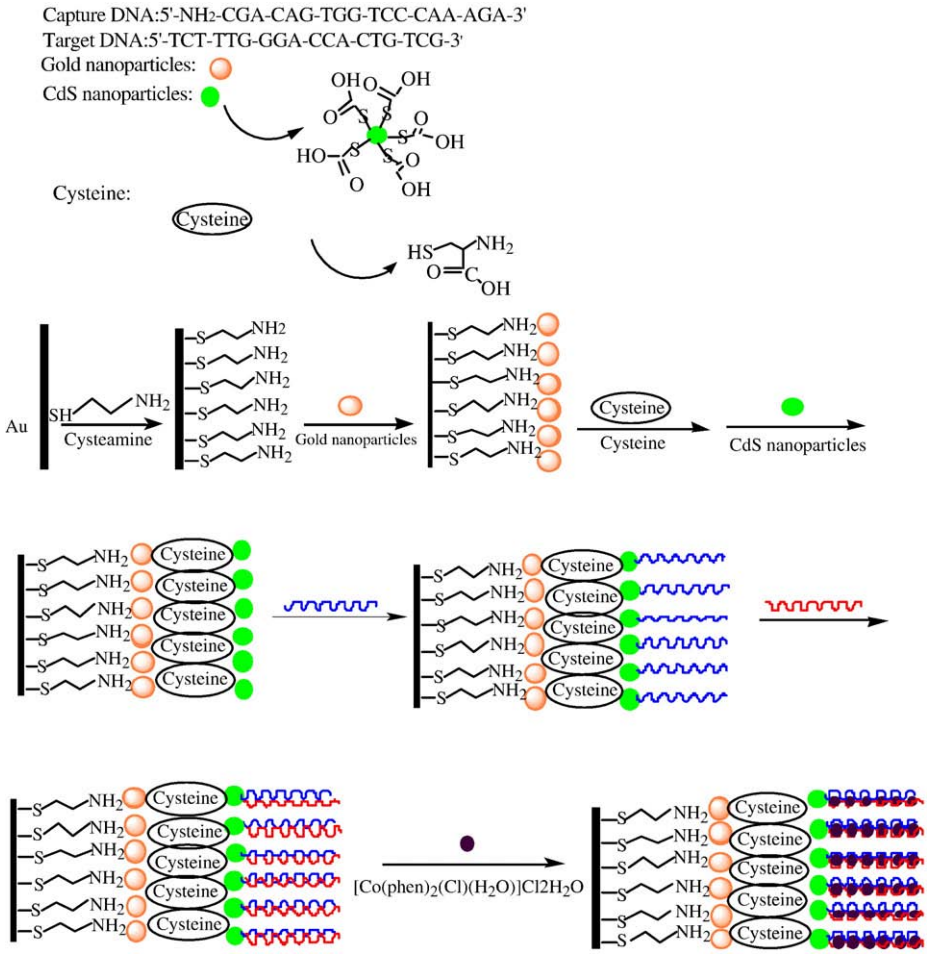

Fig. 2. Schematic diagram of the DNA biosensor fabrication.

quiet time was 2 s. In this paper, all the reported results for every electrode were the mean value from three parallel measurements.

3. Results and discussion

3.1. The fabrication principles of Au NPs and CdS NPs layers modified electrode

Fig. 2 shows the schematic diagram of the fabricated DNA biosensor. The cysteamine monolayer on gold electrode was easily obtained by a direct formation of thiol–Au bond. The prepared gold nanoparticles were negative charged due to the adsorption of protective agent of trisodium citrate on the surface and could be directly adsorbed onto the cysteamine monolayer by an electrostatic interaction with positively charged amine group of cysteamine. The cysteine monolayer assembly on gold nanoparticles surface was the same principle with that of cysteamine on gold electrode. Then, the assembly of carboxyl acid group functionalized CdS NPs on cysteine monolayer was accomplished by a protocol of EDC/NHS. In general, the carboxyl acid of CdS NPs was activated by EDC to permit coupling to available primary amines of cysteine. The immobilization of probe DNA carrying amine group onto the surface of carboxylic acid functionalized CdS NPs was further realized by the same EDC/NHS activation method.

3.2. Cyclic voltammetry of $[Fe(CN)_6^{3-/4-}]$ at the modified electrode surface

The electron transfer of ferricyanide through the modified electrode could be used as a valuable tool to monitor the whole electrode fabrication process. Fig. 3 shows the cyclic voltammograms obtained for differently modified electrodes in 2.5 mM $[Fe(CN)_6^{3-/4-}]$ aqueous solution containing 0.1 M KCl at the scan rate of 50 mV s^{-1}. The bare Au electrode witnessed a pair of well-defined redox peaks with the anodic (E_{pa}) and cathodic (E_{pc}) peak potential of 0.342 V and 0.253 V, respectively, and a peak potential difference of 89 mV (Curve a). These peaks could be

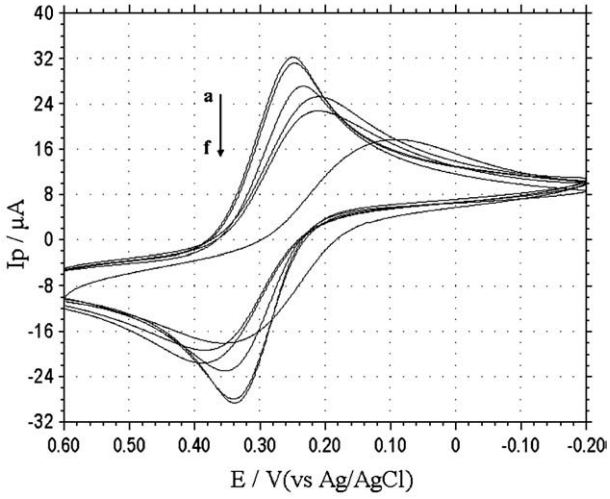

Fig. 3. Cyclic voltammograms of the bare electrode (a), and different modified electrodes with the sequential assembly of gold nanoparticles (b), cysteamine monolayer (c), CdS nanoparticles (d), ssDNA immobilization (e), and hybridization with target DNA (f), in 2.5 mM $[Fe(CN)_6^{3-/4-}]$ aqueous solution containing 0.1 M KCl.

definitely attributed to the redox behaviors of $[Fe(CN)_6^{3-/4-}]$. The self-assembly of cysteamine monolayer on electrode surface induced a small decrease of peak current, which was invoked by the diffusion inhibition of $[Fe(CN)_6^{3-/4-}]$ to the electrode surface (Curve c). The gold nanoparticles modification was convinced to enable increase the effective electrode surface area and enhance the rate of electron transfer, which was evidenced by a slight increase in the voltammetric responses of $[Fe(CN)_6^{3-/4-}]$ than that of bare electrode (Curve b). However, the further assembly of CdS NPs on the cysteine/Au NPs/Au modified electrode decreased obviously the peak current of $[Fe(CN)_6^{3-/4-}]$ as observed in curve d, which could be reasonable considering that the electron transfer of $[Fe(CN)_6^{3-/4-}]$ to the underlying electrode surface was partially blocked due to the repellence of redox species by the negative carboxyl acid group capped on CdS NPs. Curve e shows the electrochemical behavior of $[Fe(CN)_6^{3-/4-}]$ at the further probe DNA modified electrode. The peak current is much lower than that of curve d, indicating that the probe DNA has been successfully immobilized on the surface of the modified electrode and the peak current decrease could be well assigned to the repellence of $[Fe(CN)_6^{3-/4-}]$ by the negatively charged phosphate backbone of probe DNA. When the hybridization of modified electrode with target complementary DNA was proceeded, the peak current of $[Fe(CN)_6^{3-/4-}]$ was observed with a further decrease (Curve f). The introduction of complementary DNA increases the negative charge responsible for the increased repellence of redox species. On the other side, it has been revealed that the DNA immobilization and hybridization could be effectively operated on current fabricated electrode surface.

The cyclic voltammograms for probe DNA modified electrode in 10 mM PBS solution containing 2.5 mM $[Fe(CN)6^{4-}/^{3-}]$ and 0.1 M KCl with the scan rates varied from 0.05 to 0.35 V s^{-1} were investigated. It could be obtained that the peak current were proportional to the square roots of the scan rates (data not shown), which was characteristic for a typical diffusion-controlled electrochemical behavior [36].

3.3. Electrochemical impedance spectroscopy of $[Fe(CN)_6^{3-/4-}]$ at the modified electrode surface

EIS can also give further information on the impedance changes of the electrode surface during the modification process. In EIS, the semicircle diameter could represent the electron-transfer resistance, R_{et}, which dominate the electron transfer kinetics of the redox probe at the electrode interface. Fig. 4 shows the Nyquist plot of the differently modified electrodes in 0.1 M KCl solution containing 2.5 mM $K_3Fe(CN)_6/K_4Fe(CN)_6$ (1:1) at open circuit potential with the frequency varied from 0.01 Hz to 100 kHz. An almost straight line was observed for the bare Au electrode, which was typical characteristic of a mass diffusion controlled electron transfer process. The assembly of cysteamine monolayer on electrode surface induced a larger interfacial electron transfer resistance (Cuve c) as compared with that of bare Au electrode. For the Au NPs modified electrode, the R_{et} was found to be lower than that of cysteamine/Au electrode. The results could be rationalized by improved electron transfer kinetics of redox probe on nanoparticles modified electrode, the R_{et} is increased to be 2.374×10^2 Ω cm^2 with the further assembly of CdS NPs (Curve d), indicating the blocking of carboxyl acid functionalized CdS NPs to the approach of redox probe. The probe DNA immobilization on the CdS NPs/Au modified electrode make an increase of R_{et} from 4.672×10^2 to 8.199×10^2 Ω cm^2 (Curve e), which could be ascribed to the repellence of redox probe from approaching electrode surface by negative-charged phosphate skeletons of DNA. After hybridization of the ssDNA probe with the complementary ssDNA, a R_{et} increase of 1.75 times was obtained than that of the ssDNA/Au modified electrode (Curve f). This impedance change could be also used for the characterization of DNA hybridization. The impedance experiments for differently modified electrodes were in good agreement with the results by cyclic voltammetric experiments.

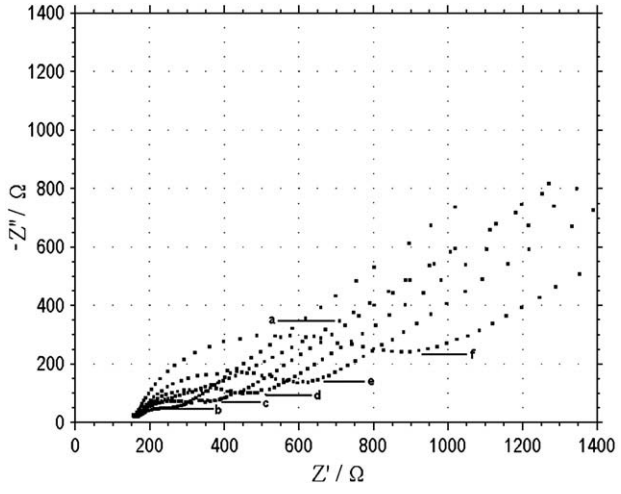

Fig. 4. EIS of the bare electrode (a), and different modified electrodes with the sequential assembly of gold nanoparticles (b), cysteamine monolayer (c), CdS nanoparticles (d), ssDNA immobilization (e), and hybridization with target DNA (f), in 2.5 mM $[Fe(CN)_6^{3-/4-}]$ aqueous solution containing 0.1 M KCl.

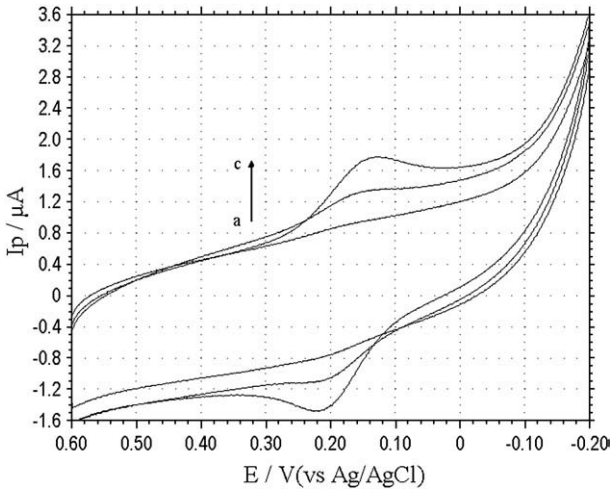

Fig. 5. Cyclic voltammograms of different modified electrodes with the exterior layer of CdS nanoparticles (a), of immobilized ssDNA (b), and hybridized dsDNA (c) in 0.2 M Tris–HCl aqueous solution (pH=6.8) after incubation in 4.0×10^{-3} M $Co(phen)_2^{2+}$ for 30 min. The initial potential was −0.20 V; the high potential was 0.60 V; the low potential was −0.20 V; the scan rate was 0.1 V s^{-1}.

3.4. The selectivity of electrochemical DNA biosensor

Fig. 5 shows the cyclic voltammograms of the CdS NPs modified Au electrode (a), ssDNA modified Au electrode (b), dsDNA modified Au electrode (c) in 0.2 M Tris–HCl aqueous solution (pH=6.8) after immersed in 0.1 mM $Co(phen)_2^{2+}$ for 30 min. It could be seen that no peaks of $Co(phen)_2^{2+}$ were observed on the CdS NPs modified Au electrode. Probe DNA immobilization on electrode surface could induce a small pair of peaks of $Co(phen)_2^{2+}$ with the anodic and cathodic potential of 0.22 and 0.15 V, respectively. This redox peaks could be attributed to the non-specific adsorption of $Co(phen)_2^{2+}$ on ssDNA by electrostatic interaction. After hybridization with target DNA, the peaks were found to be largely increased from 1.13 to 1.80 μA. The binding mode between $Co(phen)_2^{2+}$ and dsDNA could be simply considered as the intercalated interaction according to Bard [37,38] and Pang [39]. The optimum probe DNA density on the electrode surface could be obtained when at applied probe DNA concentration of 8×10^{-6} M (see Fig. S1 in the supplementary information).

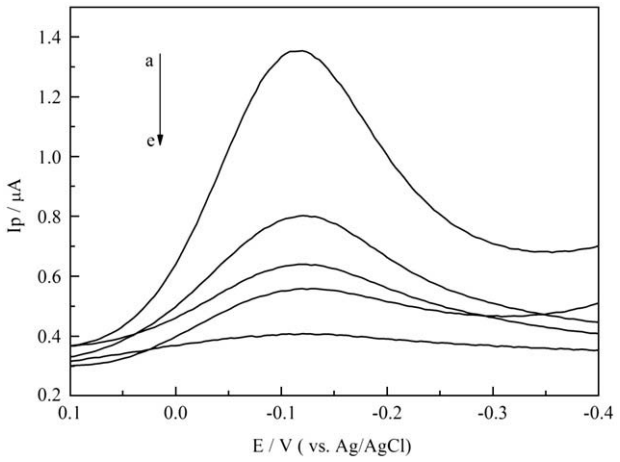

Fig. 6. DPV curves obtained in Tris–HCl aqueous solution using $Co(phen)_2^{2+}$ as an electrochemical hybridization label for detection of different DNA sequences. (a) 6.018×10^{-10} M complementary ssDNA; (b) 6.018×10^{-8} M one mismatched ssDNA; (c) capture ssDNA; (d) bare modified electrode .

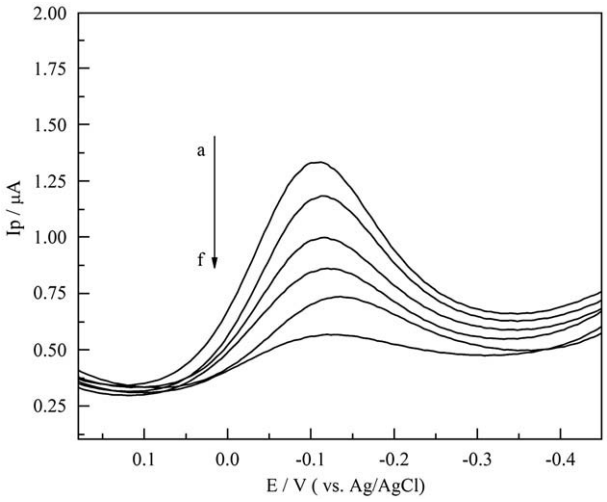

Fig. 8. The DPV signals obtained for different concentrations of target DNA: The concentration of target DNA: (a) 6.018×10^{-10} M, (b) 4.012×10^{-10} M, (c) 2.006×10^{-10} M, (d) 8.024×10^{-11} M, (e) 6.018×10^{-11} M, (f) 0.

The DPV experiments using $Co(phen)_2^{2+}$ as an electrochemical hybridization label for detection of different DNA sequence was also studied as shown in Fig. 6. Curve a, b, c, d, e were the representative DPV curves obtained in Tris–HCl aqueous solution for hybridized electrode with complementary ssDNA, one-base mismatched ssDNA, and non-complementary ssDNA sequence, probe DNA immobilized, and bare modified electrode, respectively. Each measure was performed after immersing in $Co(phen)_2^{2+}$ for 30 min. A small DPV peak current for probe DNA modified electrode indicated that $Co(phen)_2^{2+}$ has a little affinity for ssDNA on the modified electrode surface (Curve d), which was consistent with the CV results. Significant increases in the DPV signal were observed after hybridization of probe ssDNA modified electrode with the complementary ssDNA (Curve a). An obviously decreased peak current was obtained when the capture probe ssDNA was exposed to one-base mismatched ssDNA sequence in the control experiment (Curve b), and almost the same peak current for non-complementary target DNA with the solely probe DNA immobilized electrode (Curve c) showed a high selectivity of the constructed DNA biosensor for hybridization detection.

The relationship of DNA hybridization with different hybridization time was also investigated and shown in Fig. 7. It is well known that the peak current of DPV depends greatly on the hybridization time. The DPV peak current of $Co(phen)_2^{2+}$ was found to increase with the hybridization time and a maximum current response could be obtained at about 40 min.

3.5. Sensitivity of the probe DNA/CdS/Au modified electrode

The sensitivity of the electrochemical hybridization assay was further investigated by varying the target oligonucleotide concentration by differential pulse voltammetry (DPV) with the use of $Co(phen)_2^{2+}$ as an indicator. It could be seen from Fig. 8 that the DPV peak current obtained at about −0.125 V was in direct proportion to the amount of the complementary oligonucleotides varied from 1.0×10^{-8} to 2.0×10^{-10} M. The regression equation as shown in Fig. 9 was obtained as $y=1.1417x+0.9058$ (x was the concentration of the target ssDNA, M; y was ΔI_p, μA; $n=7$), and the regression coefficient of the linear curve was 0.9765. A detection limit of 2.0×10^{-11} M of the complementary oligonucleotides could be estimated using 3σ (where σ is the standard deviation of the blank solution, $n=10$). The Au nanoparticles were used to increase the assembly amount of the CdS nanoparticles and further amplify the immobilization amount of the probe DNA and enhance the performance of fabricated DNA biosensor. As compared with the results obtained by only CdS nanoparticles layer while no Au nanoparticles modified electrode (see Fig. S2 in the

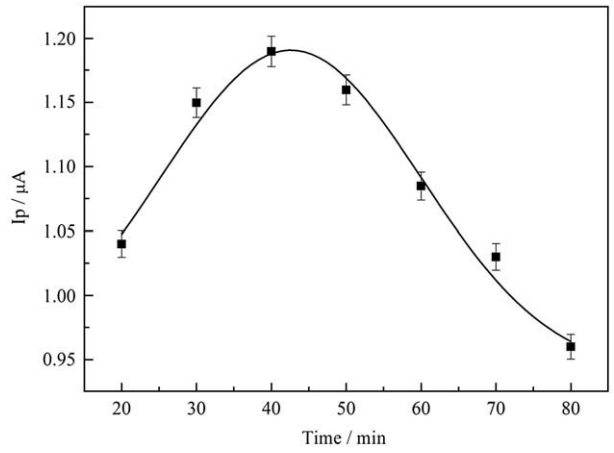

Fig. 7. Effect of hybridization time on the DPV responses of the fabricated DNA biosensor. The concentration of complementary target DNA is 2.006×10^{-9} M.

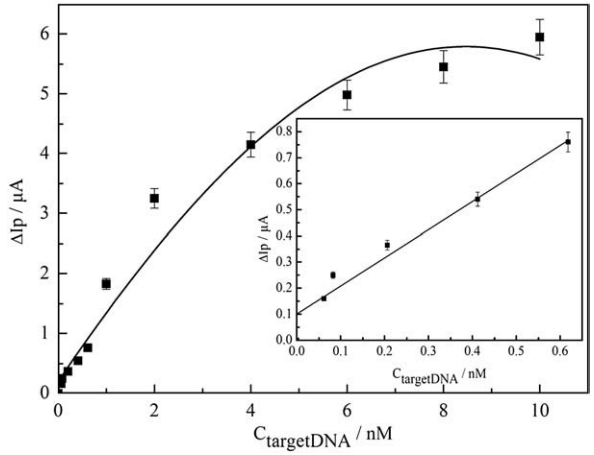

Fig. 9. The calibration curve of DPV peak current increase (ΔI_p) with different concentrations of target DNA ($C_{target\ DNA}$).

Table 1
The performance comparison of current fabricated DNA biosensor with reported in the literatures

Reference	Layers for DNA immobilization	Detection limit (mol L−1)
This method	Au and CdS NPs	2.0×10^{-11}
Ref. [40]	LBL Au NPs and MWCNTs	7.5×10^{-12}
Ref. [41]	CNTs	1.4×10^{-10}
Ref. [42]	Pt NPs and CNTs	1.0×10^{-11}
Ref. [43]	ZrO_2/SWNTs/PDC/GCE	1.38×10^{-12}
Ref. [44]	Multilayer gold nanoparticles	1×10^{-11}
Ref. [45]	Conducting polyaniline nanotube	3.759×10^{-14}
Ref. [46]	CdS nanoparticles and polypyrrole	1×10^{-9}

supplementary information), the sensitivity for detection of target DNA with the amplification of CdS and Au nanoparticles layers was increased to be about 7 times. The performance of current fabricated DNA biosensor has also been carefully compared with those reported in the literatures that used similar nanostructured materials for DNA immobilization layer and shown in Table 1. Even though the current strategy is a little bit complicated, it offered a sensitive detection of target DNA higher or comparable with those reported used different nanostructured materials including noble metal, semiconductor nanoparticles, CNTs and complex materials. Compared with some special instrumental methods like PCR, etc, it is still less sensitive, while the current electrochemical detection is of relative simplicity, low cost and satisfied sensitivity. Also, the current fabrication provided a platform to study the DNA immobilization and hybridization ability on the semiconductor nanoparticles, which was especially important for the widely application of semiconductor nanomaterials in biomolecules analysis.

3.6. Reproducibility and stability of the DNA sensor

Reproducibility of the DNA sensor was investigated with the measurement of probe DNA modified electrode in 8.024×10^{-11} M target DNA solution. Three DNA sensors, made independently, showed the response current values of 5.00×10^{-7} A, 4.95×10^{-7} A and 5.32×10^{-7} A with an acceptable variation coefficient of 3.93% ($n=3$). It indicated that a satisfactory reproducibility could be obtained by this system.

The stability of the modified electrode was also tested. No significant changes in cathodic and anodic peak current were observed for more than 10 complete CV cycles. When a modified electrode was stored in the 10 mM PBS buffer solution (pH 7.0) for at least 1 week at 4 °C, the electrode retained about 95% of its initial response.

4. Conclusion

We constructed a DNA electrochemical biosensor by immobilization Au and CdS nanoparticles on the surface of Au electrode. The Au NPs and CdS NPs could enhance the DNA immobilization and hybridization. The biosensor fabrication process were thoroughly investigated with cyclic voltammetry and EIS using $[Fe(CN)_6^{3-/4-}]$ as a electrochemical redox probe. Based on the significant difference between the voltammetric signals of $Co(phen)_2^{2+}$ obtained with ssDNA and dsDNA, the modified electrode has been applied for the detection of target DNA with $Co(phen)_2^{2+}$ as a hybridization indicator. The target DNA sequence could be quantified over the range from 2.0×10^{-10} to 1.0×10^{-8} M with a linear correlation of $r=0.9758$ and a detection limit of 2.0×10^{-11} M was achieved. The constructed DNA biosensor was established with a robust stability and good reproducibility.

Acknowledgements

This work was supported by the Natural Science Foundation of Shandong Province (No.Q2008B05), the Scientific and Technical Development Project of Qingdao (06-3-1-4-yx), and the National High-tech R&D Program (863 Program, No. 2007AA09Z113).

Appendix A. Supplementary data

Supplementary data associated with this article can be found, in the online version, at doi:10.1016/j.bioelechem.2009.01.003.

References

[1] R.F. Service, Coming soon: the pocket DNA sequencer, Science 282 (1998) 399–401.
[2] J.M. Butler, Genetics and genomics of core short tandem repeat loci used in human identity testing, J. Forensic Sci. 51 (2006) 253–265.
[3] L.M. Staudt, Gene expression physiology and pathophysiology of the immune system, Trends Immunol. 22 (2001) 35–40.
[4] G. Farace, G. Lillie, T. Hianik, P. Payne, P. Vadgama, Reagentless biosensing using electrochemical impedance spectroscopy, Bioelectrochemistry 55 (2002) 1–3.
[5] S. Reisberga, B. Piroa, V. Noela, M.C. Pham, Selectivity and sensitivity of a reagentless electrochemical DNA sensor studied by square wave voltammetry and fluorescence, Bioelectrochemistry 69 (2006) 172–179.
[6] N.L. Rosi, C.A. Mirkin, Nanostructures in biodiagnostics, Chem. Rev. 105 (2005) 1547–1562.
[7] D. Gerion, F. Chen, B. Kannan, A. Fu, W.J. Parak, D.J. Chen, A. Majumdar, A.P. Alivisatos, Room-temperature single-nucleotide polymorphism and multiallele DNA detection using fluorescent nanocrystals and microarrays, Anal. Chem. 75 (2003) 4766–4772.
[8] T.G. Drummond, M.G. Hill, J.K. Barton, Electrochemical DNA sensors, Nat. Biotechnol. 21 (2003) 1192–1199.
[9] L. He, M.D. Musick, S.R. Nicewarner, F.G. Salinas, S.J. Benkovic, M.J. Natan, C.D. Keating, Colloidal Au-enhanced surface plasmon resonance for ultrasensitive detection of DNA hybridization, J. Am. Chem. Soc. 122 (2000) 9071–9077.
[10] R.J. Lao, S.P. Song, H.P. Wu, L.H. Wang, Z.Z. Zhang, L. He, C.H. Fan, Electrochemical interrogation of DNA monolayers on gold surface, Anal. Chem. 77 (2005) 6475–6480.
[11] S. Moses, S.H. Brewer, L.B. Lowe, S.E. Lappi, L.B.G. Gilvey, M. Sauthier, R.C. Tenent, D.L. Feldheim, S. Franzen, Characterization of single- and double-stranded DNA on gold surfaces, Langmuir 20 (2004) 11134–11140.
[12] L.B. Lowe, S.H. Brewer, S. Kramer, R.R. Fuierer, G.G. Qian, C.O. Agbasi-Porter, S. Moses, S. Franzebm, D.L. Feldheim, Laser-induced temperature jump electrochemistry on gold nanoparticle-coated electrodes, J. Am. Chem. Soc. 125 (2003) 14258–14259.
[13] C.F. Ding, F. Zhao, M.L. Zhang, S.S. Zhang, Hybridization biosensor using 2, 9-dimethyl-1, 10-phenantroline cobalt as electrochemical indicator for detection of hepatitis B virus DNA, Bioelectrochemistry 72 (2008) 28–33.
[14] V. Ostatná, N. Dolinnaya, S. Andreev, T. Oretskaya, J. Wang, T. Hianik, The detection of DNA deamination by electrocatalysis at DNA-modified electrodes, Bioelectrochemistry 67 (2005) 205–210.
[15] K.R. Brown, A.P. Fox, M.J. Natan, Morphology-dependent electrochemistry of cytochrome *c* at Au colloid-modified SnO_2 electrodes, J. Am. Chem. Soc. 118 (1996) 1154–1157.
[16] L.L. Bao, S.M. Mahurin, R.G. Haire, S. Dai, Silver-doped sol–gel film as a surface-enhanced Raman scattering substrate for detection of uranyl and neptunyl ions, Anal. Chem. 75 (2003) 6614–6620.
[17] R. Ma, T. Sasaki, Y. Bando, Layer-by-layer assembled multilayer films of titanate nanotubes, Ag- or Au-loaded nanotubes and nanotubes/nanosheets with polycations, J. Am. Chem. Soc. 126 (2004) 10382–10388.
[18] S. Kidambi, J.H. Dai, J. Li, L.M. Bruening, Selective hydrogenation by Pd nanoparticles embedded in polyelectrolyte multilayers, J. Am. Chem. Soc. 126 (2004) 2658–2659.
[19] D. Li, Y. Yan, A. Wieckowska, I. Willner, Amplified electrochemical detection of DNA through the aggregation of Au nanoparticles on electrodes and the incorporation of methylene blue into the DNA-crosslinked structure, Chem. Commun. 34 (2007) 3544–3546.
[20] M. Yamada, T. Tadera, K. Kubo, H. Nishihara, Electrochemical deposition of biferrocene derivative-attached gold nanoparticles and the morphology of the formed film, J. Phys. Chem. B 107 (2003) 3703–3711.
[21] L. Zhao, A.C.L. Siu, J.A. Petrus, Z. He, K.T. Leung, Interfacial bonding of gold nanoparticles on a H-terminated Si (100) substrate obtained by electro- and electroless deposition, J. Am. Chem. Soc. 129 (2007) 5730–5734.
[22] B.K. Jena, C.R. Raj, Ultrasensitive nanostructured platform for the electrochemical sensing of hydrazine, J. Phys. Chem. C 111 (2007) 6228–6232.
[23] I. Willner, B. Willner, E. Katz, Biomolecule-nanoparticle hybrid systems for bioelectronic applications, Bioelectrochemistry 70 (2007) 2–11.
[24] Q. Xia, X. Chen, J.H. Liu, Cadmium sulfide-modified GCE for direct signal-amplified sensing of DNA hybridization, Biophys. Chem. 136 (2008) 101–107.
[25] J. Wang, G.D. Liu, A. Merkoci, Electrochemical coding technology for simultaneous detection of multiple DNA targets, J. Am. Chem. Soc. 125 (2003) 3214–3215.
[26] A. Numnuam, K.Y. Chumbimuni-Torres, Y. Xiang, R. Bash, P. Thavarungkul, P. Kanatharana, E. Pretsch, J. Wang, E. Bakker, Potentiometric detection of DNA hybridization, J. Am. Chem. Soc. 130 (2008) 410–411.
[27] E. Granot, F. Patolsky, I. Willner, Electrochemical assembly of a CdS semiconductor nanoparticle monolayer on surfaces structural properties and photoelectrochemical applications, J. Phys. Chem. B 108 (2004) 5875–5881.

[28] H.B. Yildiz, R. Freeman, R. Gill, I. Willner, Electrochemical, photoelectrochemical, and piezoelectric analysis of tyrosinase activity by functionalized nanoparticles, Anal. Chem. 80 (2008) 2811–2816.
[29] M. Zayats, A.B. Kharitonov, S.P. Pogorelova, O. Lioubashevski, E. Katz, I. Willner, Probing photoelectrochemical processes in Au–CdS nanoparticle arrays by surface plasmon resonance: application for the detection of acetylcholine esterase inhibitors, J. Am. Chem. Soc. 125 (2003) 16006–16014.
[30] R. Gill, I. Willner, I. Shweky, U. Banin, Fluorescence resonance energy transfer in CdSe/ZnS DNA conjugates: probing hybridization and DNA cleavage, J. Phys. Chem. B 109 (2005) 23715–23719.
[31] G.F. Jie, B. Liu, H.C. Pan, J.J. Zhu, H.Y. Chen, CdS nanocrystal-based electrochemiluminescence biosensor for the detection of low-density lipoprotein by increasing sensitivity with gold nanoparticle amplification, Anal. Chem. 79 (2007) 5574–5581.
[32] Z. Li, Y. Chen, X. Li, T.I. Kamins, K. Nauka, R.S. Williams, Sequence-specific label-free DNA sensors based on silicon nanowires, Nano Lett. 4 (2004) 245–247.
[33] M.M. Liang, S.L. Liu, M.Y. Wei, L.H. Guo, Photoelectrochemical oxidation of DNA by Ruthenium Tris(bipyridine) on a Tin oxide nanoparticle electrode, Anal. Chem. 78 (2006) 621–623.
[34] G. Frens, Controlled nucleation for the regulation of the particle size in monodispersed gold suspensions, Nat. Phys. Sci. 241 (1973) 20–22.
[35] Y. Zhang, Y.X. Zhu, G.L. Huang, F. Ren, F.L. Zheng, S.J. Kim, Room temperature phosphorescence from inclusion complex of β-cyclodextrin and 1-bromonaphthalene in the presence of phenol and 1-butanol, Chem. J. Chin. Univ. 22 (2001) 1397–1399.
[36] J.P. Duan, Z.F. Zhao, H.Q. Chen, G.N. Chen, A study on the electrochemical and electrochemiluminescent behavior of homogentisic acid at carbon electrodes, Electroanalysis 15 (2003) 208–218.
[37] M.T. Carter, A.J. Bard, Voltammetric studies of the interaction of tris (1,10-phenanthroline)cobalt (III) with DNA, J. Am. Chem. Soc. 109 (1987) 7528–7530.
[38] M.T. Carter, M. Rodriguez, A.J. Bard, Voltammetric studies of the interaction of metal chelates with DNA. 2. Tris-chelated complexes of cobalt (III) and iron (II) with 1,10-phenanthroline and 2,2′-bipyridine, J. Am. Chem. Soc. 111 (1989) 8901–8911.
[39] D.W. Pang, H.D. Abruna, Micromethod for the investigation of the interactions between DNA and redox-active molecules, Anal. Chem. 70 (1998) 3162–3169.
[40] H.Y. Ma, L.P. Zhang, Y. Pan, K.Y. Zhang, Y.Z. Zhang, A novel electrochemical DNA biosensor fabricated with layer-by-layer covalent attachment of multiwalled carbon nanotubes and gold nanoparticles, Electroanalysis 20 (2008) 1220–1226.
[41] S.Y. Niu, M. Zhao, R. Ren, S.S. Zhang, Carbon nanotube-enhanced DNA biosensor for DNA hybridization detection using Manganese(II)-schiff base complex as hybridization indicator, J. Inorg. Biochem. Article in press.
[42] N.N. Zhu, Z. Chang, P.G. Heb, Y.Z. Fang, Electrochemical DNA biosensors based on platinum nanoparticles combined carbon nanotubes, Anal. Chim. Acta 545 (2005) 21–26.
[43] J. Yang, K. Jiao, T. Yang, A DNA electrochemical sensor prepared by electrodepositing zirconia on composite films of single-walled carbon nanotubes and poly(2,6-pyridinedicarboxylic acid), and its application to detection of the PAT gene fragment, Anal. Bioanal. Chem. 389 (2007) 913–921.
[44] C.Y. Tsai, Y.H. Tsai, C.C. Pun1, B. Chan, T.Y. Luh, C.C. Chen, F.H. Ko, P.J. Chen, P.H. Chen, Electrical detection of DNA hybridization with multilayer gold nanoparticles between nanogap electrodes, Microsyst. Technol. 11 (2005) 1432–1858.
[45] H.X. Chang, Y. Yuan, N.L. Shi, Y.F. Guan, Electrochemical DNA biosensor based on conducting polyaniline nanotube array, Anal. Chem. 79 (2007) 5111–5115.
[46] H. Peng, C. Soeller, M.B. Cannell, G.A. Bowmaker, R.P. Cooney, J.T. Sejdic, Electrochemical detection of DNA hybridization amplified by nanoparticles, Biosens. Bioelectron. 21 (2006) 1727–1736.